YALE PEABODY MUSEUM

JOURNAL OF MARINE RESEARCH

The *Journal of Marine Research,* one of the oldest journals in American marine science, published important peer-reviewed original research on a broad array of topics in physical, biological, and chemical oceanography vital to the academic oceanographic community in the long and rich tradition of the Sears Foundation for Marine Research at Yale University.

An archive of all issues from 1937 to 2021 (Volume 1–79) are available through EliScholar, a digital platform for scholarly publishing provided by Yale University Library at https://elischolar.library.yale.edu/.

Requests for permission to clear rights for use of this content should be directed to the authors, their estates, or other representatives. The *Journal of Marine Research* has no contact information beyond the affiliations listed in the published articles. We ask that you provide attribution to the *Journal of Marine Research.*

Yale University provides access to these materials for educational and research purposes only. Copyright or other proprietary rights to content contained in this document may be held by individuals or entities other than, or in addition to, Yale University. You are solely responsible for determining the ownership of the copyright, and for obtaining permission for your intended use. Yale University makes no warranty that your distribution, reproduction, or other use of these materials will not infringe the rights of third parties.

Annual to interannual variations of $f\,CO_2$ in the northwestern Mediterranean Sea: Results from hourly measurements made by CARIOCA buoys, 1995–1997

by E. M. Hood[1,2] and L. Merlivat[1]

ABSTRACT

A time series of $f\,CO_2$, SST, and fluorescence data was collected between 1995 and 1997 by a CARIOCA buoy moored at the DyFAMed station (Dynamique des Flux Atmospheriques en Mediterranée) located in the northwestern Mediterranean Sea. On seasonal timescales, the spring phytoplankton bloom decreases the surface water $f\,CO_2$ to approximately 290 µatm, followed by summer heating and a strong increase in $f\,CO_2$ to a maximum of approximately 510 µatm. While the $\Delta f\,CO_2$ shows strong variations on seasonal timescales, the annual average air-sea disequilibrium is only 2 µatm. Temperature-normalized $f\,CO_2$ shows a continued decrease in dissolved CO_2 throughout the summer and fall at a rate of approximately 0.6 µatm d^{-1}. The calculated annual air-sea CO_2 transfer rate is -0.10 to -0.15 moles CO_2 m^{-2} y^{-1}, with these low values reflecting the relatively weak wind speed regime and small annual air-sea $f\,CO_2$ disequilibrium. Extrapolating this rate over the whole Mediterranean Sea would lead to a flux of approximately -3×10^{12} to -4.5×10^{12} grams C y^{-1}, in good agreement with other estimates. An analysis of the effects of sampling frequency on annual air-sea CO_2 flux estimates showed that monthly sampling is adequate to resolve the annual CO_2 flux to within approximately $\pm 10 - 18\%$ at this site. Annual flux estimates made using temperature-derived $f\,CO_2$ based on the measured $f\,CO_2$-SST correlations are in agreement with measurement-based calculations to within ± 7–10% (depending on the gas transfer parameterization used), and suggest that annual CO_2 flux estimates may be reasonably well predicted in this region from satellite or model-derived SST and wind speed information.

1. Introduction

The carbon dioxide cycle in the upper ocean is controlled by a combination of biological and physical processes such as upwelling, convection, the cycle of biological productivity, and responds to meteorological forcing such as gas exchange between the surface ocean and the atmosphere. The Mediterranean Sea is an area where many of these processes occur within a relatively small area (Lévy *et al.,* 1998), making it a natural laboratory for characterizing the interplay of these parameters and the response of CO_2 on a variety of timescales. Studies of CO_2 in the surface ocean have sought to explain the causes of

1. LODYC, UMR 7617, CNRS/IRD/UPMC, Tour 24, 4eme etage, 4 Place Jussieu, 75252 Paris Cedex 05, France.
2. Present address: Intergovernmental Oceanographic Commission, UNESCO, 1 rue Miollis, 75732 Paris Cedex 15, France. *email: m.hood@unesco.org*

seasonal variations along with the annual cycle of CO_2 in order to make estimates of a region's ability to act as a source or a sink to the atmosphere. More recently, it has been determined that for some areas, short-term variations (i.e., daily to weekly) in $f CO_2$ and the processes controlling surface biogeochemistry over small to mesoscale regions may contribute significantly to the annual behavior of the system (Watson *et al.,* 1991; Doney *et al.,* 1996; McGillicuddy and Robinson, 1997; Lévy *et al.,* 1998; McGillicuddy *et al.,* 1998) and these short term variations are missed by the coarse time and space scale sampling typical of most oceanographic sampling programs. Because of the temporal and spatial data coverage required for these investigations, standard oceanographic sampling methods are simply not feasible for many regions of the world's oceans, and research aimed at understanding the large-scale upper ocean CO_2 cycle must now necessarily focus on developing methods of monitoring and prediction of CO_2 in the upper ocean based on remotely-sensed information. One promising method is relating surface ocean CO_2 to other parameters such as sea-surface temperature or ocean color that can be measured via satellite (Stephens *et al.,* 1995; Wanninkhof *et al.,* 1996; Goyet and Peltzer, 1997; Bates *et al.,* 1998; Lee *et al.,* 1998; Boutin *et al.,* 1999; Hood *et al.,* 1999). These methods rely heavily on frequent measurements of a number of physical, chemical, biological, and meteorological parameters to establish the correlations over a period that is long relative to the period of interest, and as yet, no sufficiently long data set exists to determine definitively how long these relations may hold for a given region.

In this work, we present results of the CARIOCA buoy program at the DyFAMed Station in the northwestern Mediterranean Sea, which made hourly measurements of the fugacity of CO_2 ($f CO_2$), sea-surface temperature, fluorescence, and wind speed at various time periods between 1995–1997. With this data, we describe the variations of $f CO_2$ in this area on seasonal, annual, and interannual timescales, and investigate the sampling frequency necessary to adequately resolve the annual air-sea flux of CO_2, similar to the analysis presented by Bates *et al.* (1998) for the Sargasso Sea. Finally, we present correlations of $f CO_2$ and SST for the region and demonstrate how they might be used to predict surface $f CO_2$ using satellite-derived or model-derived SST data.

2. Methods

Measurements of $f CO_2$, sea-surface temperature, and fluorescence were made using a moored CARIOCA buoy (Merlivat and Brault, 1995; Lefevre *et al.,* 1993; http://www.lodyc.jussieu.fr/carioca) between May 1995 and December 1997 as part of the Dynamique des Flux Atmospheriques en Mediterranée (DyFAMed) program. This program is part of the France—Joint Global Ocean Flux Study (France—JGOFS). The DyFAMed station (Fig. 1) is located approximately 52 km southeast of Nice, France in the northwestern Mediterranean Sea at 43°25′N, 7°52′E, with a water column depth of approximately 2600 m. This region is bounded by a permanent cyclonic gyre and is sufficiently isolated from lateral transport that physical processes may be regarded in a 1-D
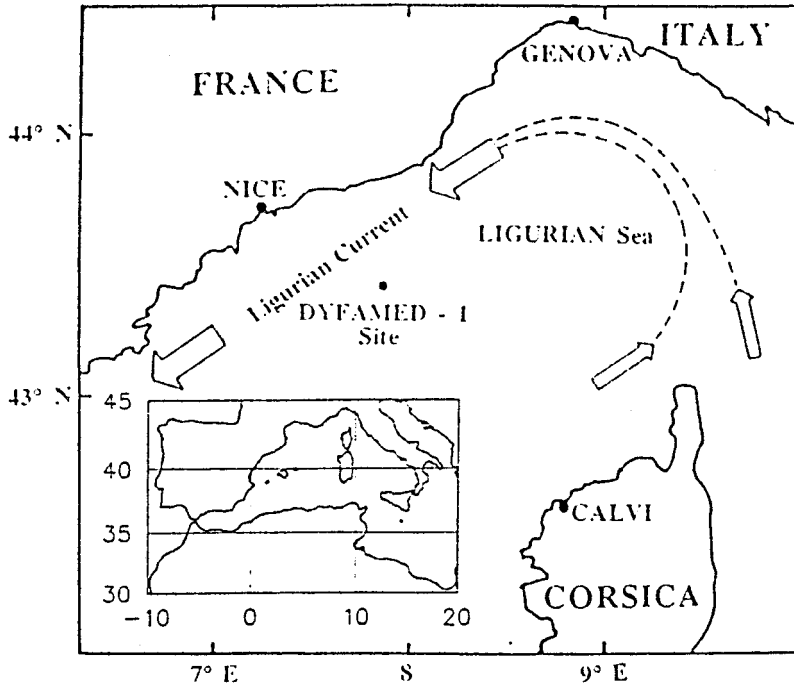
Figure 1. Location of the DYFAMED sampling site. The main cyclonic circulation is shown by the arrows. (Figure from Avril and Copin, Deep-Sea Res., 1993.)

sense (Lévy *et al.,* 1998; Andersen and Prieur, 2000). The JGOFS program at the DyFAMed station has collected a vast data set of physical, biological, and chemical parameters, and several works (Lévy *et al.,* 1998; Copin-Montégut, 2000) have well-characterized the physical and biogeochemical processes at the site.

Measurements were made by the buoy during the three years over the following periods:

1995 June 9–August 28

1996 January 16–26; March 12–April 28

1997 February 3–March 17; April 30–July 10; August 29–October 29; December 3–28.

The measurement of fCO_2 is made spectrophotometrically and is based on the optical absorbance of the pH indicator solution thymol blue diluted in seawater. Carbon dioxide in the surrounding seawater equilibrates with the indicator solution across a gas permeable (silicon) membrane in an exchanger cell, and the resulting change in optical absorbance induced by the pH change is measured by the spectrophotometer. The equation used to

calculate fCO_2 from the buoy measurement of optical absorbance (Lefevre *et al.,* 1993) is:

$$fCO_2 = \frac{k_i A_T}{\alpha k_1}\left[\frac{A_M}{A} - 1\right]\left[\frac{1 - \dfrac{C}{A_T}\dfrac{A}{A_M}}{1 + 2\dfrac{k_2}{k_i}\dfrac{A}{A_M - A}}\right] \tag{1}$$

where $A = \log(I_{810}/I_{596}) - k$ for the dye, I_{810} and I_{596} is the transmitted light through the dye at 810 and 596 nanometers, respectively, $k = \log(I_{810}/I_{596})$ *seawater* (the blank), $A_T =$ alkalinity of the dye solution in mole kg^{-1}, $A_M =$ optical absorbance of the basic form of the dye measured with the buoy spectrophotometer, $C =$ concentration of the dye in the seawater ($C = 1 \times 10^{-4}$ mole kg^{-1}), $k_i =$ dissociation constant of thymol blue dye (Zhang and Byrne, 1996) k_1 and $k_2 =$ dissociation constant of carbonate and bicarbonate in seawater used for dilution (Goyet and Poisson, 1989), and $\alpha =$ solubility coefficient (Weiss, 1974).

The spectrophotometer system is calibrated in the laboratory using a Li-Cor 6262 infrared CO_2-H_2O analyzer with calibrated gas standards. The calibration procedure and equations for calculating the various parameters as a function of optical absorbances are described in Bakker *et al.,* 2001 and in Lefevre *et al.,* 1993. Intercomparison studies between the buoys and ship-based measurements during a number of field programs (Hood *et al.,* 1999; Bates *et al.,* 2000; Bakker *et al.,* 2001; Hood *et al.,* 2001; http://www.lodyc.jussieu.fr/carioca) show agreement between the two methods to within 2 ± 5 µatm over long time periods. These values reflect uncertainty in the ship-based measurements as well as some degree of natural variability, and thus are a conservative estimate of the accuracy and precision of the buoy. Laboratory tests show a reproducibility of ± 0.5 µatm over short time periods at constant temperature (Lefevre *et al.,* 1993). During the mooring period between February and July of 1997, the sensor was calibrated before and after this 6 month period and the drift found to be $+5$ µatm. As this is within the limits of the uncertainty of the measurements, no correction was applied. The fluorescence is measured using a WETlab WETstar miniature fluorometer factory calibrated to chlorophyll-*a* content. The buoy was equipped with a RM Young Wind Monitor Jr. Propeller anemometer on a mast approximately 2 meters above the water surface, and made hourly wind speed measurements. Wind speeds were converted to 10 meter wind speeds using the bulk formula (Roll, 1965):

$$U_{10} = U_2\left(1 + \frac{C_d^{0.5}}{k}\cdot\ln\frac{10}{2}\right) \tag{2}$$

where k is the Von Karmann constant (0.4) and the drag coefficient, C_d, is assumed to be 1.1×10^{-3}.

During the three years of measurements, the wind speed data were not continuous owing to loss of anemometers. Comparisons of the buoy wind speed data with the wind speed data
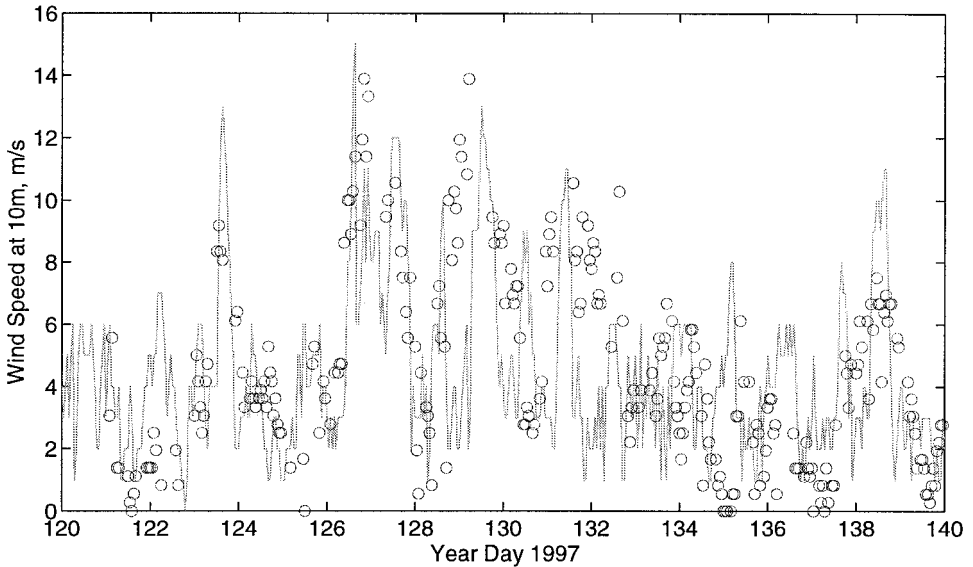
Figure 2. Comparison of wind speed data from the Météo-France weather station at Nice, France (line), and measurements made by the buoy (circles).

from the Meteo-France weather station at Nice (approximately 52 km northwest) show a mean difference of 0.3 m s^{-1} with a rmsd of about 3 m s^{-1} over an annual cycle of hourly measurements (Fig. 2). While there is quite a bit of variability on an hourly timescale, the timing and magnitude of specific wind events appears to be fairly homogeneous over this range. In order to have a continual record of wind speed, we use the Nice station wind data throughout this study.

The atmospheric fugacity of CO_2, fCO_2, which is the partial pressure corrected for nonideality of CO_2, was calculated using the equation:

$$fCO_2 \text{ air (μatm)} = X_1(P_b - P_{H_2O}) \exp[(B_{11} + 2X_2^2 \delta_{CO_2}) P/RT] \tag{3}$$

where X_1 is the mole fraction of CO_2 in dry air, P_b is the atmospheric sea level pressure, and P_{H_2O} is the vapor pressure of water at the sea surface temperature. The exponential term is the fugacity correction (Weiss, 1974), where B_{11} is the second virial coefficient for CO_2 in cm^3 mol^{-1}, δ_{CO_2} is the correction for an air-CO_2 mixture in cm^3 mol^{-1}, and X_2 is the mole fraction of the other gas components in air, equal to $1 - X_1$. The fugacity correction has a numerical value of about 0.995 to 0.998 at ambient temperatures. For atmospheric CO_2 concentrations, we use the average of the monthly concentrations measured at Lampedusa Island, 35°31′N 12°37′E, (Ciattaglia and Chamard, 1997) and Monte Cimone, Italy, 44°11′N, 10°42′E (Colombo and Santaguida, 1998). The monthly means were then linearly interpolated onto the time grid of the buoy measurements for each year. Atmospheric pressure data was obtained from the Meteo-France weather station at Nice.
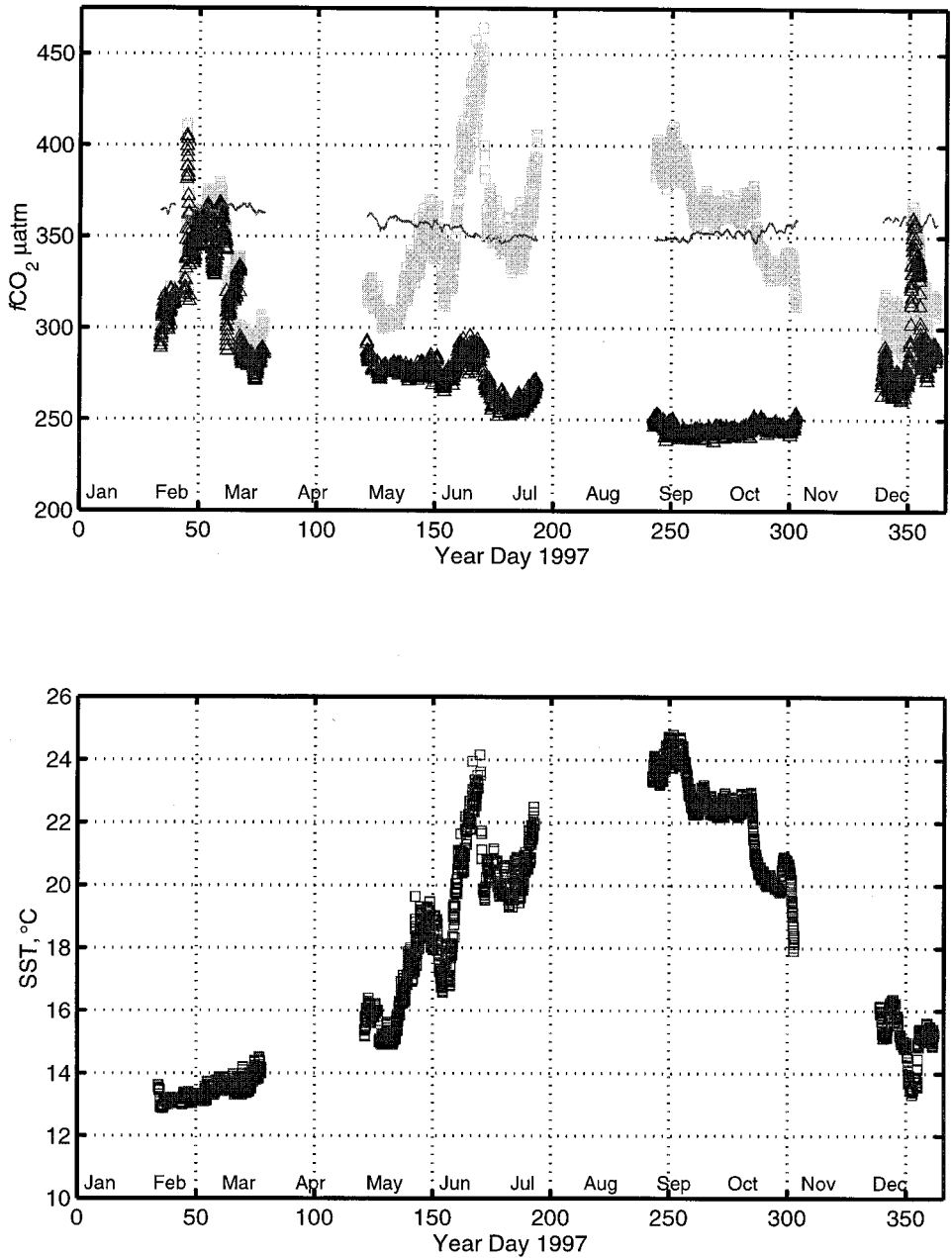
Figure 3. (a) 1997 fCO$_2$ data; fCO$_2$ are shown as gray squares, fCO$_2$ normalized to 13°C are shown as black triangles, and atmospheric fCO$_2$ is shown as a thin black line. (b) 1997 SST data. (c) 1997 fluorescence data given in relative concentration units. (d) 1997 wind speed measured by the buoy, adjusted to 10 meter heights using Eq. (2).
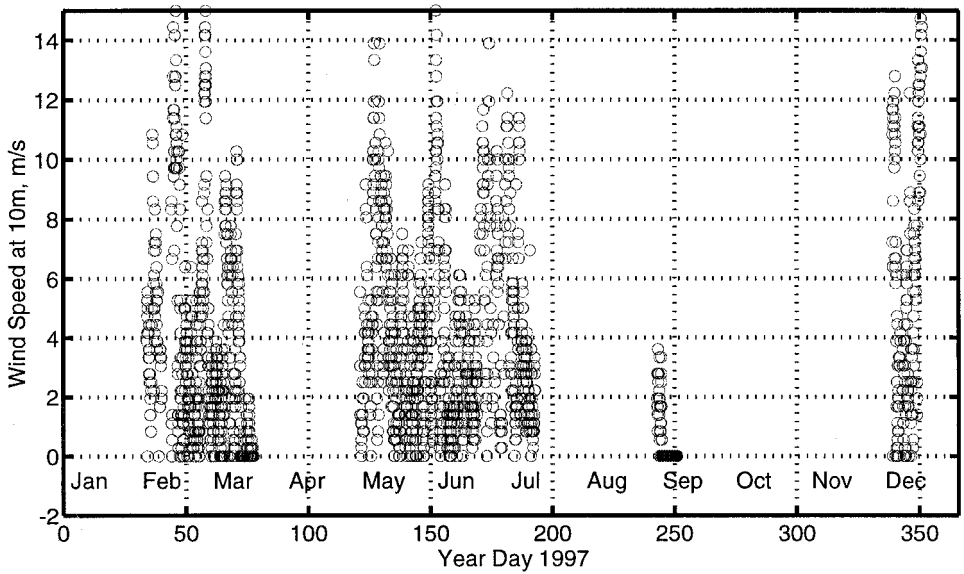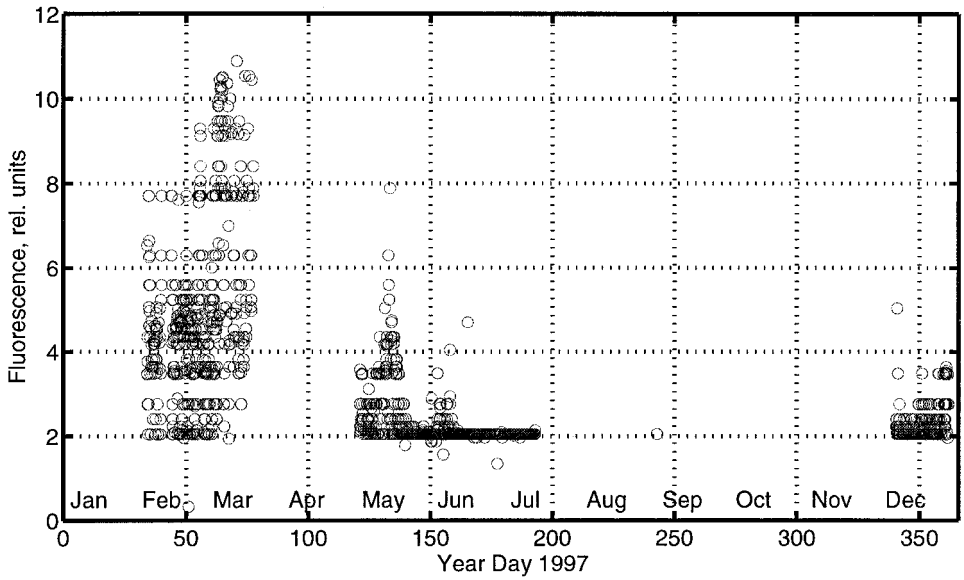
Figure 3. (Continued)

3. Annual and interannual variability

The thermal cycle at DyFAMed is characterized by a uniform winter water column at about 13°C resulting from intense vertical convection and deep water formation, with progressively shoaling isotherms through the spring and summer producing a strongly stratified water column (Lévy *et al.*, 1998). Nutrients are rapidly depleted in the surface water after the spring bloom, although the summer mixed layer is thinner than the euphotic zone, which is only partially nutrient-depleted (Copin-Montégut, 2000). In the fall, the thermocline is gradually eroded and the water column is mixed, bringing to the surface the underlying CO_2-rich 13°C water (Lévy *et al.*, 1998; Copin-Montégut, 2000). Figures 3a, 3b, 3c, and 3d show the 1997 fCO_2, SST, fluorescence, and wind speed data, respectively, measured by the buoy. In February, the base of the mixed layer is about 300 m deep and shoals to about 15–20 m in early spring, and the euphotic layer is at approximately 50 m in the summer (Lévy *et al.*, 1998). Between February and mid-March, the fCO_2 shows a strong increase followed by a rapid decrease, with fCO_2 values reaching as low as 285 µatm. Assuming that lateral advection is indeed minimal in this area, the peak in fCO_2 may be the result of vertical mixing, bringing up CO_2-rich water from below, followed by a decrease in fCO_2 as a result of increased photosynthetic activity. An increase in biological activity after about day 50 associated with the spring bloom can be seen in the fluorescence signal. From mid-April to late July the fCO_2 increases as a result of surface water warming.

The partial pressure of CO_2 in seawater is a function of the temperature, total CO_2 concentration, alkalinity, and salinity of seawater. Of these, temperature and total CO_2 concentration are the strongest influences, with changes in alkalinity and salinity only having minor effects (for a thorough review, see Takahashi *et al.*, 1993). By normalizing the fCO_2 to a constant temperature, the thermodynamic effect can be removed and changes in fCO_2 resulting from changes in total CO_2 concentration can be more easily seen. To normalize the data to a constant temperature of 13°C we use the equation of Takahashi *et al.* (1993):

$$(\partial fCO_2/\partial T)/fCO_2 = 0.0423°C^{-1}. \qquad (4)$$

The temperature-normalized fCO_2 (hereafter referred to as fCO_{2N}), also shown in Figure 3a, continues to decrease after the spring bloom throughout the summer until September. The fluorometer data (Fig. 3c) show no appreciable activity after the first part of June, while the fCO_{2N} continues to decrease slightly. Assuming that lateral advection is minimal at this location (Lévy *et al.*, 1998; Andersen and Prieur, 2000), this continued decrease in total CO_2 throughout the summer may in large part be the result of outgassing of the high fCO_2 from the warm surface water to the atmosphere. The observed rate of decrease of fCO_{2N} over this period is approximately 0.6 µatm d^{-1}. Using a mixed layer depth of 20 m (Lévy *et al.*, 1998), the gas exchange rate during this period is between 0.3 and 0.8 µatm d^{-1}, depending on whether the gas transfer rate of Liss and Merlivat (1986) or Wanninkhof (1992) is used. The December data show a rapid increase in fCO_2 and decrease in SST resulting from mixing caused by a strong wind event on day 350 followed

by rapid restratification. As winter progresses, the temperature continues to decrease until it reaches the winter minimum value of about 13°C and the water column mixes.

All three years of fCO_2, fCO_{2N}, and SST data are shown in Figures 4a, 4b, and 4c, respectively. There is remarkably good agreement and consistent temporal patterns from one year to the next in the fCO_2 and SST records between the three years with the exception of the timing of the onset of the spring bloom. The 1996 and 1997 spring blooms show very similar features, although the 1997 spring bloom occurs approximately 20 days before the 1996 bloom. This offset between the two years is also seen in the increase in SST, where the warming begins approximately 20–30 days before the decrease in fCO_2. This increase in SST is indicative of the onset of summer stratification, which initiates the spring bloom. The addition of the 1995 data shows the strong summer temperature and fCO_2 maximum not available in the 1997 data set, and the inclusion of this period shows that there is a strong outgassing of fCO_2 to the atmosphere during the summer. While the disequilibrium between the surface water and atmospheric fCO_2 (ΔfCO_2) varies strongly from a maximum of $+164$ μatm at the peak of summer to a minimum of -77 μatm in early winter and at the time of the spring bloom, the annual average ΔfCO_2 only $+2$ μatm.

4. Effects of sampling frequency on air-sea CO$_2$ flux estimates

In order to more adequately resolve fCO_2 and SST over the annual cycle, a composite year was constructed using the 1996 winter and spring bloom period, the 1997 data after the spring bloom period, and the 1995 summer data, and this composite year fCO_2, SST, and wind speed are shown in Figures 5a, 5b, and 5c, respectively. Because 1997 was the longest record, 1997 data were used where possible. However, during the spring bloom period, the 1996 data were used rather than the 1997 data because the coverage over this period was more complete in 1996. As discussed above, the variability of the fCO_2 during the bloom period is very similar between the two years. As long as the SST and wind records are kept consistent with the fCO_2 records used (i.e., 1996 wind and SST used with 1996 fCO_2), there is no difference in the annual flux estimates between a composite year using the 1996 bloom versus a composite year using the 1997 bloom. No attempt was made to establish closure of the annual cycle for this composite year, although the composite year temperature record shows a very good, albeit artificial, correspondence between December 27th, 1997 and January 16th, 1996, and attests to the regularity of the thermal cycle at this site. From this composite year, a more complete cycle of SST and fCO_2 can be seen, showing a 15°C temperature range and a 230 μatm range in fCO_2 over the annual cycle. These data from the composite year were interpolated onto the hourly time grid of the wind data from the Meteo-France Nice station and linearly interpolated over missing data points. The number of days not measured in the composite year is 95. To extrapolate the record to the full year, the ends of the time series were padded using the nearest measured data point; i.e., January 1st through January 15th were set equal to the first values measured on January 16th, and December 28th through December 31st were set equal to the last values measured on December 27th.
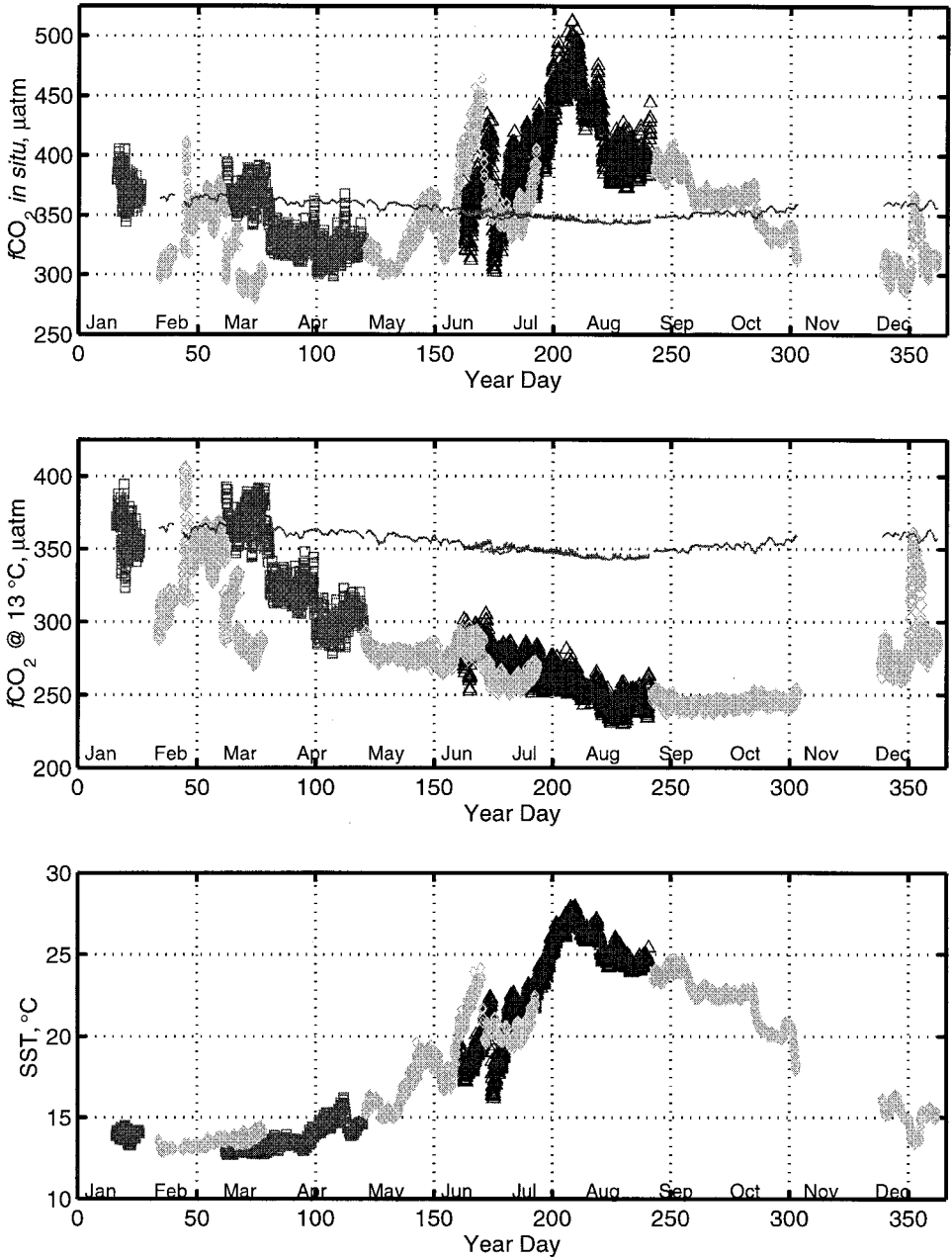
Figure 4. (a) fCO_2 data from all three years; 1995 = dark triangles, 1996 = medium gray squares, and 1997 = light gray diamonds. (b) Temperature-normalized fCO_2 data from all three years; symbols are the same as for (a). (c) Sea-surface temperature data from all three years.

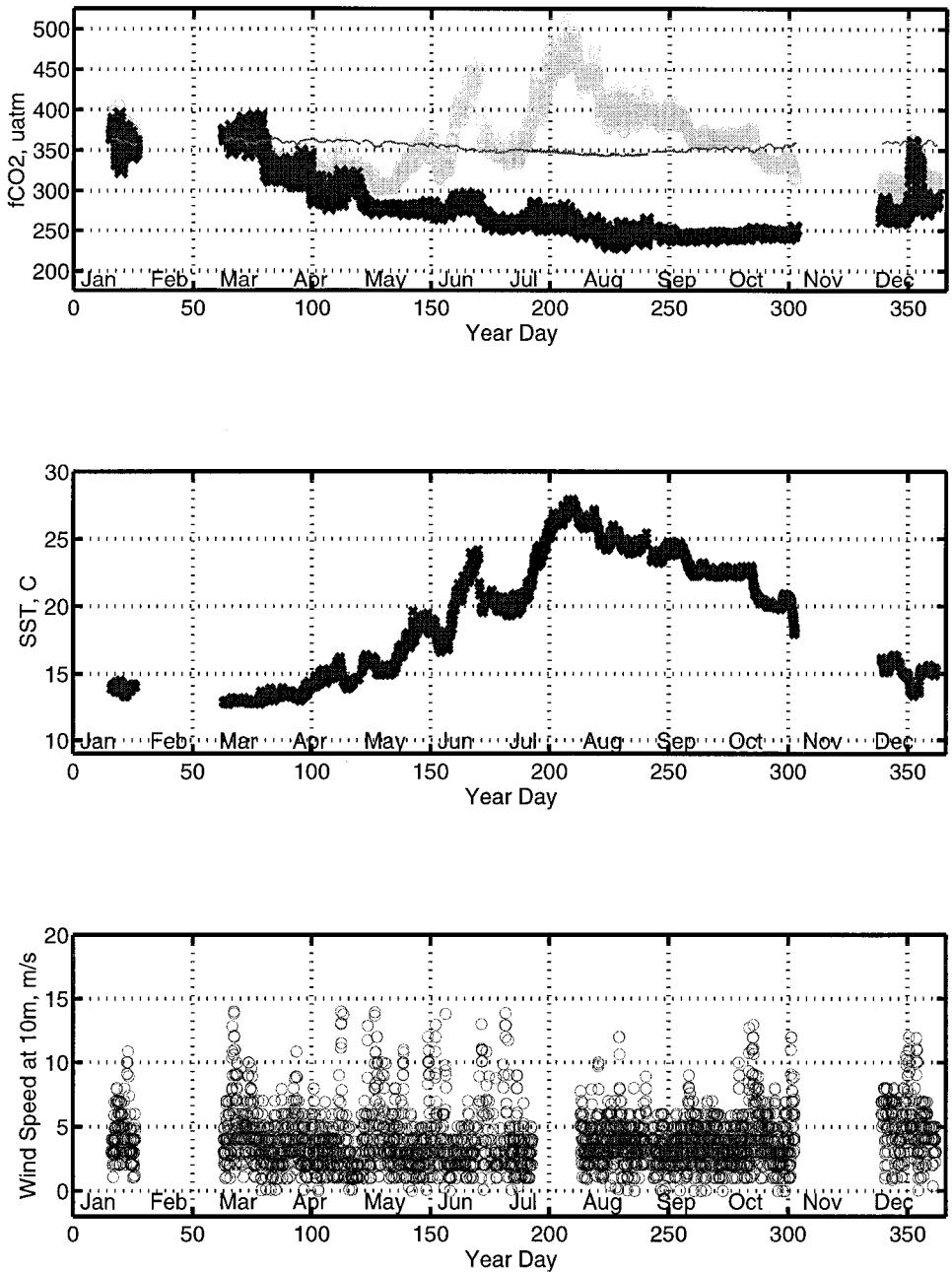Figure 5. (a) The composite year $f\mathrm{CO}_2$ data. $f\mathrm{CO}_2$ at *in situ* temperatures $=$ light gray circles, $f\mathrm{CO}_2$ at 13°C $=$ dark crosses, and atmospheric $f\mathrm{CO}_2$ $=$ thin line. (b) The composite year SST data. (c) The composite year wind data.

The air-sea flux of CO_2 over this composite year was calculated using the basic flux equation:

$$F = k \, \alpha \Delta f CO_2 \tag{5}$$

where k is the gas transfer velocity (parameterized as a function of the wind speed and the Schmidt number of the gas), α is the solubility coefficient (Weiss, 1974), and $\Delta f CO_2$ is the partial pressure gradient between the water and atmosphere. For the gas transfer velocity, k, we use the formulations of Liss and Merlivat (1986) and Wanninkhof (1992). A negative flux implies flux from the atmosphere into the water. The annual flux calculated is between -0.10 and -0.15 mol m^{-2} y^{-1}, using the Liss and Merlivat (1986) or Wanninkhof (1992) gas transfer formulation, respectively. Extrapolating this rate over the Mediterranean Sea using a surface area of 2.5×10^{12} m^2 leads to a flux of between -2.5×10^{11} and -3.8×10^{11} moles CO_2 y^{-1}. This is in good agreement with the earlier work of Copin-Montégut (1993), who estimated an annual uptake of approximately -3.5×10^{11} moles CO_2 y^{-1} based on an average $f CO_2$ in the surface waters and average annual wind speed.

Using an approximately 17-month time series of $f CO_2$ measurements made in the Sargasso Sea near Bermuda, Bates *et al.* (1998) present an analysis to determine the frequency of surface sampling needed to adequately resolve annual air-sea flux of CO_2 and found only a $\pm 10\%$ difference between estimates made using monthly sampling versus sampling every three to four days. They further suggest that monthly sampling should be adequate to resolve annual CO_2 fluxes in other areas. To test this, we simulated a program of monthly sampling and compared flux estimates made using these measurements with those made using all available data. Monthly sampling was simulated in two ways; first, by taking the average of three days of hourly sampling at monthly intervals as might be done during an oceanographic field program having monthly sampling at a given site over a year, and secondly, by using the average of only one day of hourly sampling to represent the month as done by Bates *et al.* Each set of calculations was performed three times, varying the choice of days used each month to avoid any biases in 'sampling.' The data points from each month were then interpolated over the annual cycle using the hourly time grid of the wind speed data, and the ends of the time series extrapolated to the full year using the nearest end values as described for the measured data. This creates an annual record of hourly estimates from which the annual flux is then calculated. The differences of the hourly $f CO_2$ estimates between the one-day sampling period and the three-day sampling period are small, but show significant differences when compared to the measured hourly data. A comparison of the record from the 1 day/month sampling strategy and the hourly measurements from the buoy (composite year) are shown in Figure 6.

Table 1 shows the results of this analysis. The annual fluxes calculated from monthly sampling are within ± 10–18% of those calculated using the hourly measurements, with the estimates using the gas transfer formulation of Wanninkhof (1992) having slightly larger differences resulting from the stronger dependence of the calculated flux on the wind speed. The rmsd between the estimated hourly $f CO_2$ values and the measured values,
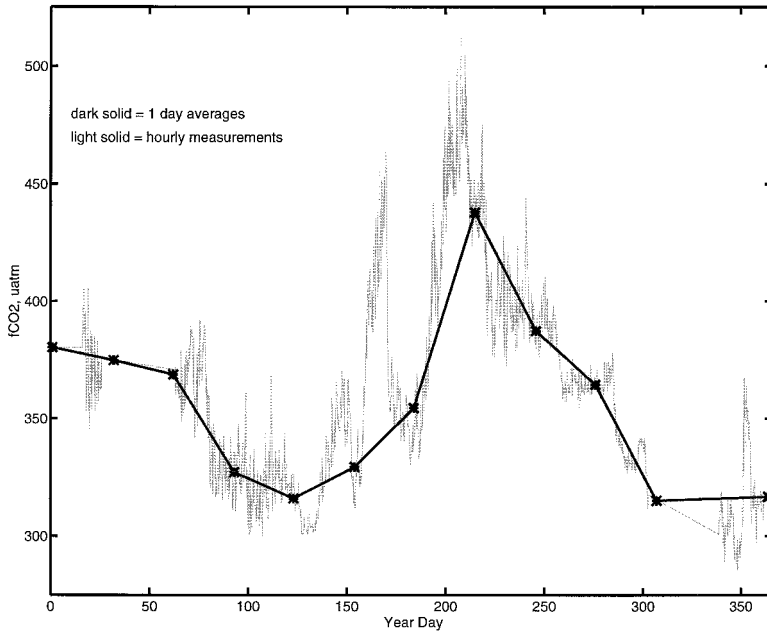
Figure 6. Comparison of hourly measurements (light gray line) with simulated monthly sampling (dark line with points).

however, is quite large, owing to the fact that the monthly sampling with simple linear interpolation between the data points misses a great deal of natural variability. By shifting the choice of days for one and three day averages/month, the annual flux calculations changed by less than 7%. This may, however, be fortuitous, as most of the large-scale variability occurred in the summer when wind speeds are relatively low and the flux less important.

Bates *et al.* report a ±10% difference between measurements made on average every three to four days versus monthly sampling. Areas such as Bermuda and the northwestern Mediterranean having low to moderate wind speed regimes are the most amenable regions for this sort of extrapolation and these analyses suggest that for certain areas, monthly sampling may be adequate to resolve the annual air-sea fluxes to ±10–20%. However, as noted by Bates *et al.,* the caveat is that the uncertainty resulting from the different gas

Table 1. Annual air-sea fluxes of CO_2 at Dyfamed. The root mean squared deviations (rmsd) between the 1 and 3 day sampling periods/month and the hourly measurements are given in parentheses.

	Liss and Merlivat (1986) $\text{mol m}^{-2}\,\text{y}^{-1}$	Wanninkhof (1992) $\text{mol m}^{-2}\,\text{y}^{-1}$
Hourly	−0.10	−0.15
Monthly, 3 day means	−0.10 (rmsd = 0.3)	−0.17 (rmsd = 0.5)
Monthly, 1 day means	−0.11 (rmsd = 0.3)	−0.18 (rmsd = 0.5)

transfer parameterizations, where the calculated transfer velocities vary by approximately a factor of 2, is much larger than differences in any of the estimation techniques used.

5. fCO_2-SST correlations

While monthly sampling may be adequate to resolve air-sea CO_2 fluxes in some areas, even this coarse resolution of sampling is not feasible for many areas of the ocean over long time periods. To overcome the lack of observational data in many areas and to allow for continuous monitoring, increasing emphasis is being placed on the use of satellite-derived or model-derived information to estimate surface ocean CO_2. One promising technique is to use measurement-based correlations of fCO_2 and SST with satellite-derived SST and wind speed data to make estimates of fCO_2 and air-sea CO_2 flux over larger temporal and spatial scales (Hood *et al.,* 1999; Boutin *et al.,* 1999; Lee *et al.,* 1998; Bates *et al.,* 1998; Goyet and Peltzer, 1997; Wanninkhof *et al.,* 1996; Stephens *et al.,* 1995).

On annual timescales, surface water fCO_2 at DyFAMed is predominantly controlled by temperature, whereas shorter timescales show the influence of biological processes and mixing, particularly in the spring and winter periods. Therefore, the year was resolved into seasonal components using the changes in SST and fCO_2 from the composite year as indicators of these seasonal changes. The fCO_2-SST correlations for the composite year are shown in Figure 7. The equation used to describe the correlations has the form

$$y = ax^2 + bx + c \tag{6}$$

where a, b, and c are the coefficients of the relation and x represents SST. The coefficients and uncertainties were calculated using the Levenberg-Marquardt method for nonlinear regression, and are shown in Table 2. The degree of scatter in the fits to the data results from natural interannual variability in the composite year used for the analysis as well as difficulty in precisely resolving the spring and winter periods using only SST, which varies over a very small range during the period when mixing or biological processes cause fCO_2 to vary substantially.

The estimated fCO_2 using these correlations and the SST data from the composite year are shown in Figure 8. The major features of the annual cycle are reasonably well resolved, and the root-mean-squared deviation (rmsd) between the estimated values and the measurements is ± 12 µatm. Table 3 shows the comparisons between annual and seasonal measurements and estimates of fCO_2 as well as a comparison of fluxes calculated using each for the composite year. The annual and seasonal means of the estimated values are in good agreement with the measurements, although the rmsd for each period indicate that these estimates are not without considerable uncertainty. However, at DyFAMed, as with many regions of the oceans, the air-sea flux is dominated by wind speed rather than the air-sea concentration differences of fCO_2, the flux estimates using the estimated values of fCO_2 agree with the measured values to within ± 7–10% over the annual cycle for the composite year.

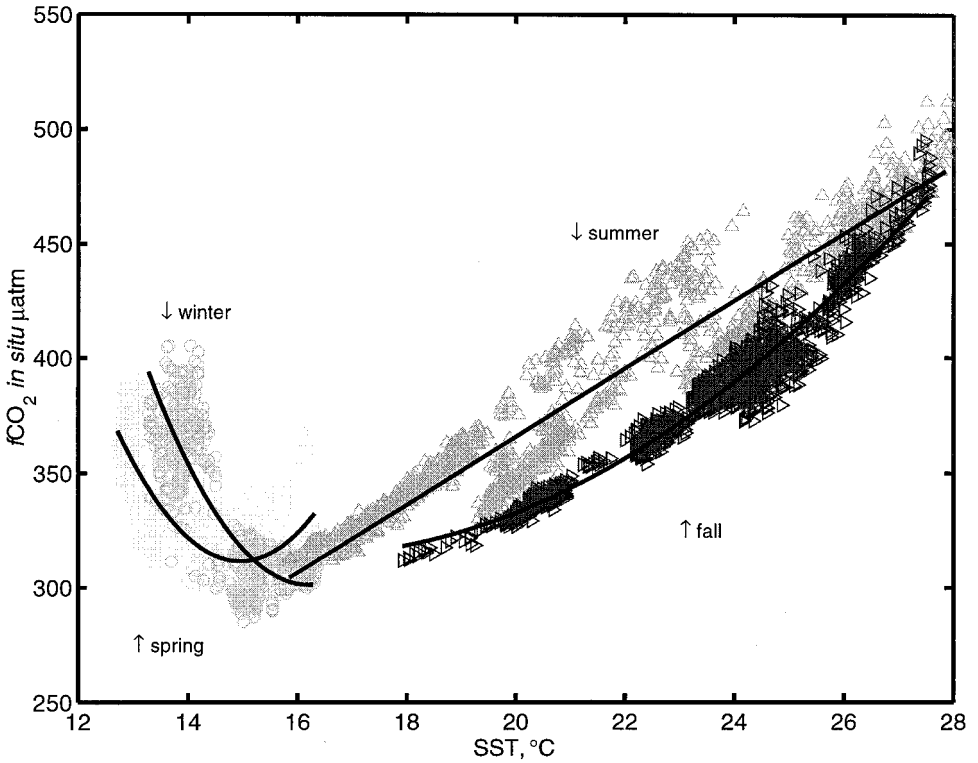We also use the composite year algorithms to predict the fCO_2 for the individual years.

Figure 7. fCO_2-SST correlations from the composite year. Spring (March to mid-May) = light gray circles; Winter (mid-December to the end of January) = medium gray circles; Summer (mid-May to August) = medium gray triangles; Fall (August to mid-December) = dark triangles. The solid lines are the nonlinear least squares regressions for each season.

Taking the longest of the available records (1997), we also calculate the annual flux to estimate how well the composite algorithms do at predicting other years. This is not an ideal comparison, however, since the composite year data consists mostly of the 1997 data, and the 1997 data do not cover the entire year. It is thus necessary to linearly interpolate between missing data points to create and annual record for comparison. The comparisons between the estimated and measured fluxes for 1997 are much poorer than for the

Table 2. Coefficients of the seasonal fCO_2-SST correlations. The data used for the winter period are from mid-December to the end of January; spring data are from March to mid-May; Summer data are from mid-May to August; Fall data are from August to mid-December.

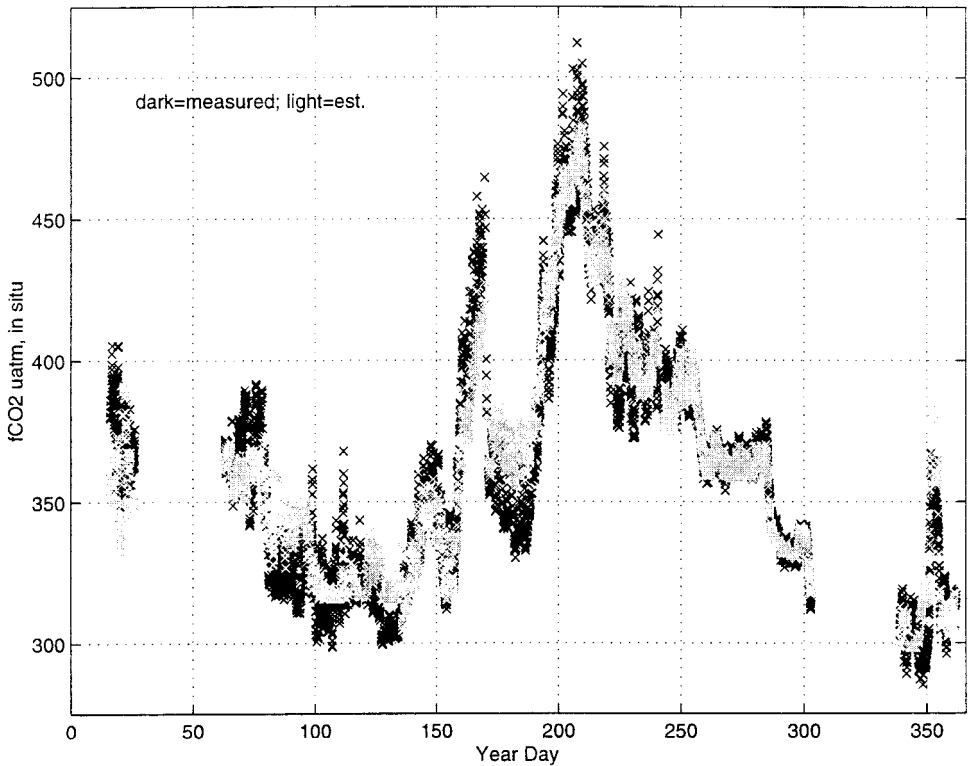|	a	σ_a	b	σ_b	c	σ_c
Winter	11	1	−350	34	3140	253
Spring	11.3	0.5	−337	14	2834	96
Summer			14.8	0.1	70	3
Fall	1.19	0.03	−38	2	618	17

Figure 8. Comparison of measured $f\text{CO}_2$ data from the composite year (dark) to the estimated $f\text{CO}_2$ (light) using the $f\text{CO}_2$-SST correlations.

Table 3. Annual and seasonal $f\text{CO}_2$ measurements and estimates. The mean annual and seasonal $f\text{CO}_2$ and fluxes are shown for measurements and estimates using the $f\text{CO}_2$-SST correlations. The root mean squared deviation (rmsd) between the measured and estimated values is shown for each season. The fluxes are calculated using both the Liss and Merlivat (1986) gas transfer formulation (first number) and the Wanninkhof (1992) formulation (second number). The numbers in parentheses in the 1997 row show the results of the comparisons without the spring bloom period.

	Measured $f\text{CO}_2$ µatm	Estimated $f\text{CO}_2$ µatm	rmsd µatm	Correlation coefficient (r)	Measured flux mol m^{-2} y^{-1}	Estimated flux mol m^{-2} y^{-1}
Annual	365	365	±12	0.96	−0.10, −0.15	−0.11, −0.16
Winter	335	331	±18	0.83	−0.47, −0.80	−0.44, −0.77
Spring	333	336	±15	0.79	−0.22, −0.47	−0.18, −0.40
Summer	387	387	±14	0.96	−0.03, −0.03	−0.03, −0.03
Fall	380	379	±6	0.98	+0.17, +0.40	+0.16, +0.37
1995 annual	405	403	±13			
1996 annual	345	343	±17			
1997 annual	346	350	±21 (11)		−0.17, −0.30 (−0.15), (−0.24)	−0.12, −0.21 (−0.12), (−0.19)

composite year and seasons, although they agree to within $\pm 20\%$ when the spring bloom period is not included (bracketed values in table).

It is difficult to assess the efficacy of algorithms to estimate fCO_2 and flux in light of the limited number of appropriate data sets for a single area and the large uncertainties in the gas transfer velocity formulations. However, these results suggest that at least for annual flux estimates in this region of the Mediterranean Sea, the use of measurement-based algorithms and satellite-derived information may provide reasonable annual flux estimates with uncertainties that are small relative to other uncertainties affecting air-sea gas exchange calculations. An annual time series from another year (or years) is needed to verify the utility of the composite algorithm developed in this study before any definitive conclusions may be drawn about the utility of this technique.

6. Summary and conclusions

A time series of fCO_2, SST, and fluorescence data measured between 1995 and 1997 by a moored CARIOCA buoy at the DyFAMed station in the northwestern Mediterranean Sea was presented, and the causes of the annual and seasonal variability in surface fCO_2 discussed. A series of analyses were performed to determine if monthly sampling of fCO_2 in this area would be adequate to resolve annual fluxes of fCO_2 as was shown for the Sargasso Sea by Bates *et al.* (1998), and results suggest that the annual flux may be estimated from monthly sampling to within ± 10–20% of that calculated based on hourly measurements when extrapolated over the full year. To determine if SST could be used as a proxy to calculate fCO_2 in the surface waters, and thus estimate fluxes using satellite or model-derived SST and wind speed data, correlations between fCO_2 and SST were established for each season and used to estimate fCO_2 and the air-sea flux of CO_2. The results based on the composite year show that the annual fCO_2 may be predicted with an uncertainty of ± 12 µatm, and the annual flux to within $\pm 10\%$ of that calculated using direct measurements. A more thorough data set is needed to test these algorithms for predicting other years, but the initial results suggest that the annual flux can be predicted to within ± 10–20% for another year.

This work supports the suggestion of Bates *et al.* (1998) that for some regions, monthly sampling of surface fCO_2 seems adequate to resolve annual air-sea flux estimates, and also supports previous work (Stephens *et al.,* 1995; Wanninkhof *et al.,* 1996; Goyet and Peltzer, 1997; Bates *et al.,* 1998; Lee *et al.,* 1998; Boutin *et al.,* 1999; Hood *et al.,* 1999) demonstrating the potential of using fCO_2-SST correlations to estimate surface water fCO_2 in some areas of the world's oceans once the initial measurement-based correlations have been established. It still remains to be seen how long these correlations remain useful for a given region, which will require a consecutive multi-year, temporally well-resolved time series of data from a single location.

for this project. The authors also wish to thank Jacky Lanoiselle for his engineering aid and at-sea work for the buoy program.

REFERENCES

Andersen, V. and L. Prieur. 2000. One-month study in the open NW Mediterranean Sea (DYNAPROC experiment, May 1995): overview of the hydrobiogeochemical structures and effects of wind events. Deep-Sea Res. I, *47,* 397–422.

Bakker, D. C. E., J. Etcheto, J. Boutin and L. Merlivat. 2001. Variability of surface-water $f CO_2$ during seasonal upwelling in the equatorial Atlantic Ocean as observed by a drifting buoy. J. Geophys. Res. (in press).

Bates, N. R., L. Merlivat, L. Beaumont and C. Pequignet. 2000. Intercomparison of shipboard and moored CARIOCA buoy seawater measurements in the Sargasso Sea. Mar. Chem. *72,* 239–255.

Bates, N. R., T. Takahashi, D. W. Chipman and A. H. Knap. 1998. Variability of $p CO_2$ on diel to seasonal timescales in the Sargasso Sea near Bermuda. J. Geophys. Res., *103,* 15567–15585.

Boutin, J., J. Etcheto, Y. Dandonneau, D. C. E. Bakker, R. A. Freely, H. Y. Inoue, M. Ishii, R. D. Ling, P. D. Nightengale, N. Metzl and R. Wanninkhof. 1999. Satellite sea surface temperature: A powerful tool for interpreting *in situ* $p CO_2$ measurements in the equatorial Pacific Ocean. Tellus, *51B,* 490–508.

Ciattaglia, L. and P. Chamard. 1997. Monthly and annual atmospheric CO_2 record from flask measurements at Lampedusa Island, Italy, *in* Trends: A Compendium of Data on Global Change. Carbon Dioxide Information Analysis Center, Oak Ridge National Laboratory, Oak Ridge, TN, http://cdiac.esd.ornl.gov.

Colombo, T. and R. Santaguida. 1998. Atmospheric CO_2 record from *in situ* measurements at Mt. Cimone, *in* Trends: A Compendium of Data on Global Change. Carbon Dioxide Information Analysis Center, Oak Ridge National Laboratory, Oak Ridge, TN, U.S.A., http://cdiac.esd.ornl.gov.

Copin-Montégut, C. 1993. Alkalinity and carbon budgets in the Mediterranean Sea. Global Biogeochem. Cycles, *7,* 915–925.

—— 2000. Consumption and production on scales of a few days of inorganic carbon, nitrate and oxygen by the planktonic community. Results of continuous measurements at the Dyfamed Station in the northwestern Mediterranean Sea (May 1995). Deep-Sea Res. I, *47,* 447–477.

Doney, S. C., D. M. Glover and R. G. Najjar. 1996. A new coupled, one-dimensional biological-physical model for the upper ocean: Applications to the JGOFS Bermuda Atlantic Time-series Study (BATS) site. Deep-Sea Res. II, *43,* 591–624.

Goyet, C. and E. T. Peltzer. 1997. Variations of CO_2 partial-pressure in surface seawater in the equatorial Pacific Ocean. Deep-Sea Res. I, *44,* 1611–1625.

Goyet, C. and A. Poisson. 1989. New determination of carbonic acid dissociation constants in seawater as a function of temperature and salinity. Deep-Sea Res., *36,* 1635–1654.

Hood, E. M., L. Merlivat and T. Johannessen. 1999. Variations of $f CO_2$ and air-sea flux of CO_2 in the Greenland Sea gyre using high-frequency time-series data from CARIOCA drift-buoys. J. Geophys. Res., *104,* 20571–20583.

Hood, E. M., R. Wanninkhof and L. Merlivat. 2001. Short timescale variations of $f CO_2$ in a North Atlantic warm core eddy: Results from the GASEX-98 CARbon Interface OCean Atmosphere (CARIOCA) buoy data. J. Geophys. Res., *106,* 2561–2572.

Lee, K., R. Wanninkhof, T. Takahashi, S. Doney and R. Feely. 1998. Low interannual variability in recent oceanic uptake of atmospheric carbon dioxide. Nature, *396,* 155–159.

Lefevre, N., J. P. Ciabrini, G. Michard, B. Brien, M. Duchaffaut and L. Merlivat. 1993. A new optical sensor for $p CO_2$ measurement. Mar. Chem., *42,* 189–198.

Lévy, M., L. Mémery and J. M. André. 1998. Simulation of primary production and export fluxes in the Northwestern Mediterranean Sea. J. Mar. Res., *56,* 197–238.

Liss, P. S. and L. Merlivat. 1986. Air-sea gas exchange rates: Introduction and synthesis, *in* The Role of Air-Sea Exchange in Geochemical Cycling, P. Buat-Menard, ed., D. Reidel, Dordrecht, Holland, 113–127.

McGillicuddy, D. J. and A. R. Robinson. 1997. Eddy-induced nutrient supply and new production in the Sargasso Sea. Deep-Sea Res. I, *44,* 1427–1450.

McGillicuddy, D. J. Jr., A. R. Robinson, D. A. Siegel, H. W. Jannasch, R. Johnson, T. D. Dickey, J. McNeil, A. F. Michaels and A. H. Knap. 1998. Influence of mesoscale eddies on new production in the Sargasso Sea. Nature, *394,* 263–265.

Merlivat, L. and P. Brault. 1995. CARIOCA buoy: Carbon dioxide monitor. Sea Techn., *10,* 23–30.

Roll, H. U. 1965. Physics of the Marine Atmosphere, International Geophysics Series, Vol. 7, Academic Press.

Stephens, M. P., G. Samuels, D. B. Olson, R. A. Fine and T. Takahashi. 1995. Sea-air flux of CO_2 in the North Pacific using shipboard and satellite data. J. Geophys. Res., *100,* 13,571–13,583.

Takahashi, T., J. Olafsson, J. G. Goddard, D. W. Chipman and S. C. Sutherland. 1993. Seasonal variation of CO_2 and nutrients in the high-latitude surface oceans: A comparative study. Global Biogeochem. Cycles, *7,* 843–878.

Wanninkhof, R. 1992. Relationship between wind speed and gas exchange over the ocean. J. Geophys. Res., *97,* 7373–7382.

Wanninkhof, R., R. A. Freely, H. Chen, C. Cosca and P. P. Murphy. 1996. Surface water fCO_2 in the eastern equatorial Pacific during the 1992–1993 El Nino. J. Geophys. Res., *101,* 16,333–16,343.

Watson, A. J., C. Robinson, J. E. Robinson, P. J. Williams and M. J. R. Fasham. 1991. Spatial variability in the sink for atmospheric carbon dioxide in the North Atlantic. Nature, *350,* 50–53.

Weiss, R. F. 1974. Carbon dioxide in water and seawater: The solubility of a non-ideal gas. Mar. Chem., *2,* 203–215.

Zhang, H. and R. H. Byrne. 1996. Spectrophotometric pH measurements of surface seawater at *in-situ* conditions: absorbance and protonation behavior of thymol blue. Mar. Chem., *52,* 17–25.